Eddies connect the tropical Atlantic Ocean and the Gulf of Mexico

Minghai Huang[1], Xinfeng Liang[1*], Yingli Zhu[1], Yonggang Liu[2], Robert H. Weisberg[2]

1. School of Marine Science and Policy, University of Delaware, Lewes, DE 19958
2. College of Marine Science, University of South Florida, St. Petersburg, FL 33701

* Corresponding to: xfliang@udel.edu

Key Points

- Some eddies from the Atlantic Ocean can ultimately reach the Gulf of Mexico and affect the Loop Current.
- Freshwater of Amazon and Orinoco River origin and other materials trapped in eddies could reach the Gulf of Mexico.
- Weakening and strengthening of the long-propagating eddies are mostly related to the variation of bathymetry.

Abstract

Numerical circulation modeling and observational studies have been conducted to understand the Loop Current (LC) system behaviors in the Gulf of Mexico (GoM). One of the factors that may influence the LC are upstream eddies from within the Caribbean Sea. By combining satellite altimetry, sea surface salinity and ocean color data, we demonstrate that mesoscale eddies from the western tropical Atlantic Ocean can eventually make their way to the Gulf of Mexico and affect the LC. In addition, our study shows that freshwater of Amazon and Orinoco River origin trapped within mesoscale eddies can also enter the GoM affecting the GoM stratification. This study provides insights into understanding variations of the LC system and showcases the roles of mesoscale eddies in connecting the open ocean and regional seas.

Plain Language Summary

The Loop Current (LC) is the dominant large-scale oceanic process in the Gulf of Mexico (GoM). However, the mechanism for variations of the LC system is still unsolved. Here, we show that some mesoscale eddies originated in the tropical Atlantic Ocean can pass through the Caribbean Sea and eventually enter the GoM. These remotely generated eddies could be an important upstream factor affecting the behavior of the LC. Also, freshwater and other materials (chlorophyll) trapped in the eddies could reach the GoM as well. In addition to advancing the understanding of the LC system, this study provides an explicit example showing eddies can serve as a route connecting regional seas and the open ocean.

1. Introduction

The Gulf of Mexico (GoM) is a semi-enclosed sea connecting the Caribbean Sea and the Atlantic Ocean through the Yucatan Channel and the Straits of Florida, respectively. The Loop Current (LC) is the most prominent physical feature in the GoM. It has a significant influence on various processes in the GoM, such as dispersal of spilled oil (e.g., Crone & Tolstoy, 2010; Liu et al., 2011; Hazen et al., 2016; Weisberg et al., 2016; Weisberg et al., 2017), sediment transport, fish production (e.g., Hazen et al., 2016), distribution of nutrients (e.g., Hu et al., 2005). In addition, it plays an essential role in the atmosphere-ocean coupling, which influence the prediction of hurricanes and their impacts (e.g., Shay & Jacob, 2006; Sheng et al., 2010; Chen & Curcic, 2016; Curcic & Chen, 2016).

The past few decades have provided a large number of observational and numerical circulation modeling studies on the LC system (e.g., Sturges & Leben, 2000; L.-Y. Oey et al., 2005; Xu et al., 2013; Chang & Oey, 2010, 2013; Liu et al., 2016; Weisberg & Liu, 2017; J. Candela et al., 2019; Hirschi et al., 2019). Despite these and others, a fundamental question remains: what controls the trajectory of the LC (Committee on Advancing Understanding of Gulf of Mexico Loop Current Dynamics, 2018)? Many factors affecting this complex, dynamical system have been proposed, such as the Yucatan channel transport, bottom topography, and atmospheric forcing. In particular, several modelling studies suggest that upstream factors outside of the GoM could be important (Murphy et al., 1999; Lie-Yauw Oey, 2004; Jouanno et al., 2008; Alvera-Azcárate et al., 2009).

Previous studies suggest that mesoscale eddies that may impact the GoM could originate as far upstream as the North Brazil Current (NBC). Rings that are shed from the NBC as it retroflects into the North Equatorial Countercurrent (NECC) can propagate northwestward and interact with

65 the Lesser Antilles. Such NBC rings may be deflected or defracted by the island chain, with the
66 result that some of these may enter the Caribbean Sea (Fratantoni & Richardson, 2006).
67 Numerical modeling studies (e.g., Murphy et al., 1999) show that potential vorticity from NBC
68 rings reforming west of the Lesser Antilles may then grow in the Caribbean Sea gaining energy
69 via mixed barotropic and baroclinic instabilities. Some of those eddies can then enter the GoM
70 through the Yucatan Channel, perhaps impacting the trajectory of the LC and the related eddy-
71 shedding process. Besides the modeling studies, drifter track, altimetry observations and Amazon
72 river plume studies also show the advection of these rings and its filaments cross Lesser Antilles
73 (e.g., Carton & Chao, 1999; Fratantoni & Richardson, 2006; Richardson, 2005; Goni & Johns,
74 2001; Chérubin & Richardson, 2007; Avera-Azcarate et al., 2009). However, more definitive
75 studies on such long-distance mesoscale eddy connections between the GoM and the tropical
76 Atlantic Ocean remain to be accomplished.

77 In this study, using various satellite products, including altimetry, sea surface salinity and
78 chlorophyll, we explore roles of mesoscale eddies in connecting the tropical Atlantic and the
79 GoM and their impacts on the LC. The paper is organized as follows. A brief description of the
80 data is provided in section 2. Section 3 presents the propagations of eddies from the tropical
81 Atlantic Ocean to the GoM. At last, the results are summarized and discussed in section 4.

82 **2. Data and Methods**

83 The daily satellite altimetry dataset from the Copernicus Marine Environment Monitoring
84 Service (CMEMS, https://marine.copernicus.eu/) was used to tack the propagation of eddies. The
85 dataset covers the period from January 1993 to December 2018 and has a spatial resolution of
86 0.25° × 0.25°. This dataset includes a number of variables, including sea level anomalies (SLA),

absolute dynamic topography (ADT) and geostrophic currents. Note that the SLA is referenced to a 20-year (1993-2012) mean (Pujol et al., 2016).

Mesoscale eddy trajectory from January 1993 to January 2018 produced by CMEMS was also used. This product provides eddy trajectory information, including type, position, amplitude (i.e., magnitude of the height difference between the extremum of SLA within the eddy and the SLA around the contour defining the eddy perimeter) and speed. Note that the eddy trajectory in this dataset will be stopped if there is land between two consecutive eddies, likely resulting in discontinuities for long-propagating eddies when they encounter topography like island chains.

To avoid the discontinuities related to the eddy detection methods mentioned above, we also examined the propagation of mesoscale eddies along a 60-cm sea surface height (SSH) isoline, which is roughly the mean of the eddy trajectories in the study region (Figure 1a). In order to examine the evolution of the eddies as they propagate, we also calculated amplitude of the mesoscale eddies along the same isoline using a 3° × 0.5° moving box (green boxes in Fig. 1).

The sea surface salinity (SSS) from European Space Agency Earth Explorer mission (SMOS) was used to explore the impacts of mesoscale eddies on the freshwater transport. The SSS data cover a period from January 2010 to December 2017 (Boutin et al., 2018). The SSS data have a temporal interval of four days and a spatial resolution of about 25 km. In addition, we examined the chlorophyll data from GlobColour, which merges several products from SeaWiFS, MERIS, MODIS, VIIRS NPP, OLCI-A, VIIRS JPSS-1 and OLCI-B to achieve better spatial and temporal coverage (Maritorena et al., 2010). The dataset is from 1997 to 2019 with a spatial resolution of 4 km and a temporal resolution of 8 days. Also, we used ETOPO5 bathymetry data examine the impacts of bathymetry on the propagating mesoscale eddies.

3. Results

The trajectories of mesoscale eddies that last more than 60 days in the study region are shown in Figure 1a-b. From the western tropical Atlantic Ocean to the GoM, the eddy trajectories are continuous except for three regions: Lesser Antilles, Chibcha Channel and Yucatan Channel. The main pattern of the anticyclonic and cyclonic eddy track is similar, and the numbers of the anticyclonic and cyclonic eddies are roughly the same. Note that since we consider the long-distance propagation of mesoscale eddies, only eddies lasting more than 60 days are presented.

Since the eddy detection method used to generate the trajectory data arbitrarily stopped the trajectory if land was found between consecutive eddies, the discontinuity shown in Figure 1a-b could be misleading. We then drew a line from the tropical Atlantic to the GoM (Fig 1) to track the propagations of mesoscale eddies and examine if the eddies on the two sides of the discontinuous locations are actually connected. Following the line, the Hovmöller diagram of sea level anomalies (SLA) (as in Alvera-Azcarate et al., 2009) is derived and shown in Figure 1c. Here, for better visualization we only present a few years of the data and the other years show similar patterns. It is clear that the eddy connection shown in Figure 1a-b is also revealed in the Hovmöller plot (Fig. 1c). In addition, many SLA signals now appear propagating continuously from the western tropical Atlantic Ocean to the GoM even in the discontinuity regions shown in Figure 1a-b. Along the line, SLA signals on the two sides of the Lesser Antilles are closely related, displaying a significant correlation of 0.69 with a time lag of 1 month, indicating some eddies inside the Caribbean Sea, particularly those originate near the Lesser Antilles are likely related to eddies in the tropical Atlantic Ocean.

We also explored the propagation of individual eddies. Three cases of long-distance eddy propagation from the western tropical Atlantic Ocean to the GoM are presented in Figure 2. For

case 1 (Figure 2a-b), we firstly see a clearly defined eddies in the middle of the tropical Atlantic Ocean in July 2014. The eddy then propagated westward until encountered the continent of the South America around October 2014. Then, the eddy propagated northwestward following the corridor along the north Brazil coastline and eventually encounter the Lesser Antilles (Figure 2a), where the intensity of the eddy was significantly reduced. However, after part of the eddy was diffracted into the Caribbean Sea in March 2014, the eddy eventually grew into a much stronger eddy as it propagated into the eastern Caribbean Sea in October 2015. At last, the eddy entered the GoM and became part of the LC in January 2016 (Figure 2b). The long-distance propagation from the middle of the tropical Atlantic Ocean to the GoM takes about 17 months. Similar to case 1, the eddy shown in case 2 (Figure 2c) was first identified in the western tropical Atlantic Ocean in March 2014, and after about 14 months it eventually entered the GoM. It should be noted that eddies originated in the western tropical Atlantic can also enter the Caribbean Sea but fail to reach the GoM. Case 3 (Figure 2d) is such an example. Therefore, the evolution of the eddies along their trajectory, which involves a number of complex dynamics (e.g., Murphy et al., 1999; Jouanno et al., 2008), deserves some further analysis.

We further examined the evolution of the eddy along their propagation trajectory (Figure 3a). When crossing the Lesser Antilles, the eddies are relatively weak with an amplitude of ~5 cm. When the eddies reach the eastern Caribbean Sea, the amplitude sharply increased to 20-25 cm. After that, the eddies intensity decreased again around the Chibcha Channel. To confirm if this evolution of eddy intensity is robust or not, we calculated the statistical results of all the detected cyclonic and anticyclonic eddies along the line shown in Figure 1. The results reveal similar but more detailed features to the three individual eddies (Figure 3b). Note that the magnitude of the amplitude is different since it is derived from the SLA trajectory dataset which is the same from

the previous individual cases. In general, the amplitude of the eddies decreases sharply when reaching the Lesser Antilles, the Chibcha Channel and the Yucatan Channel and increases when moving away from these large topographic features.

The eddy cases and the SLA propagation indicate that in contrast to the previous studies, mesoscale eddies from the tropical Atlantic Ocean, at least some of them, can cross the discontinuity regions and can finally reach the GoM. These eddies served as vorticity flux passing the Yucatan Channel could trigger the Loop Current retraction, extension and eddy-shedding. Previous studies suggest that the negative (anticyclonic) vorticity flux is related to the Loop Current extension while the positive (cyclonic) vorticity flux causes retraction and sometimes shedding (Candela et al., 2002; Lie-Yauw Oey, 2004; Athie et al., 2012). Our case eddies shown in Figure 2a-c are examples of the anticyclonic eddies inducing LC extension events.

The eddies under consideration carried other material properties along with energy and momentum. Figure 4 shows the Hovmöller diagram of the SSS anomalies and the accompanied SLA anomalies. Similar to the SLA anomalies, the SSS anomalies can translate from the NBC region, across the Lesser Antilles and into the Caribbean Sea. This is important because the barrier layers created by the fresh Amazon-Orinoco River plume, by raising SST, can contribute to Atlantic hurricane intensification (K. Balaguru et al., 2012, 2020; Ffield, 2007), and the eddies play an important role on the freshwater transport (Fournier et al., 2017). One can see the transport across Lesser Antilles even there are some data missing in the Lesser Antilles. In some years, such as 2013-2016, these SSS features can also translate cross the Chibcha and the Yucatan channels to enter the GoM. The green box marked in Fig. 4 show several such cases, which also includes two specific eddy cases in Figure 2a-c. The phases of SSS and SLA agree

179 well with each other, confirming that individual eddies can carry freshwater from western
180 tropical Atlantic Ocean to not only the Caribbean Sea as suggested by previous studies
181 (Hellweger & Gordon, 2002) but also further into the GoM.

182 In addition, chlorophyll and colored dissolved organic matter (CDOM) also show the
183 propagation of the mesoscale eddies (Hu et al., 2004; Fratantoni & Glickson, 2002). The contrast
184 between the high nutrient Amazon-influenced water and the surrounding relatively low nutrient
185 midocean water mark the NBC retroflection and the rings. The low-chlorophyll rings core and
186 high-chlorophyll boundaries show the evolution and propagation of the NBC rings. Here, the
187 propagation of chlorophyll is shown in Fig. 5. For example, from 2005 to 2006, the chlorophyll
188 anomalies propagate from the NBC retroflection regions, cross the Lesser Antilles into the
189 Caribbean Sea, and then finally into GoM. It should be noted that the mechanisms for the
190 chlorophyll anomaly are complex and are at least from two parts: horizontal advection and
191 vertical upwelling of nutrient or chlorophyll itself (Killworth et al., 2004; O'Brien et al., 2013).
192 Variability in river discharge and the numbers of the rings will also impact the chlorophyll.
193 Nevertheless, our results at least show the mesoscale eddies can affect the bio-productivity along
194 their long-propagation trajectory that connects the tropical Atlantic Ocean and the GoM.

195 **4. Conclusions and Discussion**

196 By combining the SSHA, eddy track, SSS, chlorophyll data, we show that some of the mesoscale
197 eddies originating in the tropical Atlantic Ocean can eventually enter the GoM and affect the LC.
198 In other words, mesoscale eddies can connect the tropical Atlantic Ocean and the GoM.
199 Although such a long-distance connection by way of mesoscale eddies has been suggested in
200 previous numerical studies (Murphy et al., 1999; van Westen et al., 2018), here we provide direct
201 observational evidence. In addition, earlier studies have suggested that the potential vorticity flux

through the Yucatan Channel may influence the LC trajectory and the eddy shedding process in the GoM (Murphy et al., 1999; Candela et al., 2002; Lie-Yauw Oey, 2004; Athie et al., 2012), these long distance translating eddies from the tropical Atlantic Ocean may play a role in LC evolution and LCE shedding. Besides the eddies shown along the line in Figure 1a, eddy translation along a zonal line in the Atlantic Ocean was also examined (not shown). Consistent feature translation from the Atlantic Ocean to the Caribbean Sea is seen, suggesting that such eddy connections between the Atlantic Ocean and the GoM are quite common.

A more specific impact of those long-propagating eddies is related to the freshwater transport. As the largest oceanic rings, the NBC rings transport freshwater and other materials particularly considering that the NBC flows past the Amazon River (Fratantoni & Glickson, 2002; Hellweger & Gordon, 2002; Chérubin & Richardson, 2007; Grodsky et al., 2015; Fournier et al., 2017). Early studies show that the Amazon river plume can influence the Caribbean Sea salinity variation through salt advection (Muller-Karger et al., 1988; Hellweger and Gordon, 2002). In this study, we show that Amazon and Orinoco river freshwater trapped by the mesoscale eddies can not only get into the Caribbean Sea but can finally enter the GoM in many cases (Figure 4).

There is similarity between the evolution and propagation of individual ocean eddy and of the atmosphere hurricane and storm, which also show weakening and strengthening along their trajectories. But the number of studies on the ocean counterpart of hurricanes and storms are much less. In this study, we show a close relationship between topography and variations of eddy intensity between the Lesser Antlilles and the Yucatan Channel. However, inside the GoM and in the Tropical Atlantic Ocean, no such clear relations appear. These observations suggest that various factors and mechanisms involved in any successful eddy connection events between the

tropical Atlantic and the GoM, and more carefully designed studies are needed in the future to further explore this complex dynamical process.

Acknowledgements

The work was supported by the Gulf of Mexico Research Initiative through Grant G-231804. All the data used in this study are publicly available. The altimetry and mesoscale eddy trajectory datasets can be obtained from the Copernicus Marine Environment Monitoring Service (CMEMS, https://marine.copernicus.eu/). The sea surface salinity dataset is from the European Space Agency Earth Explorer mission (SMOS, https://earth.esa.int/web/guest/missions/esa-operational-eo-missions/smos). And the chlorophyll dataset is available at GlobColour (https://hermes.acri.fr/).

Reference

1. Alvera-Azcárate, A., Barth, A., & Weisberg, R. H. (2009). The Surface Circulation of the Caribbean Sea and the Gulf of Mexico as Inferred from Satellite Altimetry. *Journal of Physical Oceanography*, *39*(3), 640–657. https://doi.org/10.1175/2008JPO3765.1
2. Athié, G., Candela, J., Ochoa, J., & Sheinbaum, J. (2012). Impact of Caribbean cyclones on the detachment of Loop Current anticyclones: WESTERN CARIBBEAN CYCLONES. *Journal of Geophysical Research: Oceans*, *117*(C3), n/a-n/a. https://doi.org/10.1029/2011JC007090
3. Balaguru, K., Chang, P., Saravanan, R., Leung, L. R., Xu, Z., Li, M., & Hsieh, J.-S. (2012). Ocean barrier layers' effect on tropical cyclone intensification. *Proceedings of the National Academy of Sciences*, *109*(36), 14343–14347. https://doi.org/10.1073/pnas.1201364109
4. Balaguru, Karthik, Foltz, G. R., Leung, L. R., Kaplan, J., Xu, W., Reul, N., & Chapron, B. (2020). Pronounced Impact of Salinity on Rapidly Intensifying Tropical Cyclones. *Bulletin of the American Meteorological Society*, *101*(9), E1497–E1511. https://doi.org/10.1175/BAMS-D-19-0303.1
5. Boutin, J., Vergely, J. L., Marchand, S., D'Amico, F., Hasson, A., Kolodziejczyk, N., et al. (2018). New SMOS Sea Surface Salinity with reduced systematic errors and improved variability. *Remote Sensing of Environment*, *214*, 115–134. https://doi.org/10.1016/j.rse.2018.05.022
6. Candela, J., Ochoa, J., Sheinbaum, J., López, M., Pérez-Brunius, P., Tenreiro, M., et al. (2019). The Flow through the Gulf of Mexico. *Journal of Physical Oceanography*, *49*(6), 1381–1401. https://doi.org/10.1175/JPO-D-18-0189.1
7. Candela, Julio, Sheinbaum, J., Ochoa, J., Badan, A., & Leben, R. (2002). The potential vorticity flux through the Yucatan Channel and the Loop Current in the Gulf of Mexico: VORTICITY FLUX AND THE LOOP CURRENT. *Geophysical Research Letters*, *29*(22), 16-1-16–4. https://doi.org/10.1029/2002GL015587

8. Carton, J. A., & Chao, Y. (1999). Caribbean Sea eddies inferred from TOPEX/POSEIDON altimetry and a 1/6° Atlantic Ocean model simulation. *Journal of Geophysical Research: Oceans*, *104*(C4), 7743–7752. https://doi.org/10.1029/1998JC900081

9. Chang, Y.-L., & Oey, L.-Y. (2010). Why Can Wind Delay the Shedding of Loop Current Eddies? *Journal of Physical Oceanography*, *40*(11), 2481–2495. https://doi.org/10.1175/2010JPO4460.1

10. Chang, Y.-L., & Oey, L.-Y. (2013). Coupled Response of the Trade Wind, SST Gradient, and SST in the Caribbean Sea, and the Potential Impact on Loop Current's Interannual Variability*. *Journal of Physical Oceanography*, *43*(7), 1325–1344. https://doi.org/10.1175/JPO-D-12-0183.1

11. Chen, S. S., & Curcic, M. (2016). Ocean surface waves in Hurricane Ike (2008) and Superstorm Sandy (2012): Coupled model predictions and observations. *Ocean Modelling*, *103*, 161–176. https://doi.org/10.1016/j.ocemod.2015.08.005

12. Chérubin, L. M., & Richardson, P. L. (2007). Caribbean current variability and the influence of the Amazon and Orinoco freshwater plumes. *Deep Sea Research Part I: Oceanographic Research Papers*, *54*(9), 1451–1473. https://doi.org/10.1016/j.dsr.2007.04.021

13. Committee on Advancing Understanding of Gulf of Mexico Loop Current Dynamics, Gulf Research Program, & National Academies of Sciences, Engineering, and Medicine. (2018). *Understanding and Predicting the Gulf of Mexico Loop Current: Critical Gaps and Recommendations* (p. 24823). Washington, D.C.: National Academies Press. https://doi.org/10.17226/24823

14. Crone, T. J., & Tolstoy, M. (2010). Magnitude of the 2010 Gulf of Mexico Oil Leak. *Science*, *330*(6004), 634–634. https://doi.org/10.1126/science.1195840

15. Curcic, M., Chen, S. S., & Özgökmen, T. M. (2016). Hurricane-induced ocean waves and stokes drift and their impacts on surface transport and dispersion in the Gulf of Mexico. *Geophysical Research Letters*, *43*(6), 2773–2781. https://doi.org/10.1002/2015GL067619

16. Ffield, A. (2007). Amazon and Orinoco River Plumes and NBC Rings: Bystanders or Participants in Hurricane Events? *Journal of Climate*, *20*(2), 316–333. https://doi.org/10.1175/JCLI3985.1

17. Fournier, S., Vandemark, D., Gaultier, L., Lee, T., Jonsson, B., & Gierach, M. M. (2017). Interannual Variation in Offshore Advection of Amazon-Orinoco Plume Waters: Observations, Forcing Mechanisms, and Impacts: AMAZON-ORINOCO PLUME ADVECTION. *Journal of Geophysical Research: Oceans*, *122*(11), 8966–8982. https://doi.org/10.1002/2017JC013103

18. Fratantoni, D. M., & Glickson, D. A. (2002). North Brazil Current Ring Generation and Evolution Observed with SeaWiFS. *JOURNAL OF PHYSICAL OCEANOGRAPHY*, *32*, 17.

19. Fratantoni, D. M., & Richardson, P. L. (2006). The Evolution and Demise of North Brazil Current Rings*. *Journal of Physical Oceanography*, *36*(7), 1241–1264. https://doi.org/10.1175/JPO2907.1

20. Goni, G. J., & Johns, W. E. (2001). A census of North Brazil Current Rings observed from TOPEX/POSEIDON altimetry: 1992-1998. *Geophysical Research Letters*, *28*(1), 1–4. https://doi.org/10.1029/2000GL011717

21. Grodsky, S. A., Johnson, B. K., Carton, J. A., & Bryan, F. O. (2015). Interannual Caribbean salinity in satellite data and model simulations. *Journal of Geophysical Research: Oceans*, *120*(2), 1375–1387. https://doi.org/10.1002/2014JC010625

22. Hazen, E. L., Carlisle, A. B., Wilson, S. G., Ganong, J. E., Castleton, M. R., Schallert, R. J., et al. (2016). Quantifying overlap between the Deepwater Horizon oil spill and predicted bluefin tuna spawning habitat in the Gulf of Mexico. *Scientific Reports*, *6*(1), 33824. https://doi.org/10.1038/srep33824

23. Hellweger, F. L., & Gordon, A. L. (2002). Tracing Amazon River water into the Caribbean Sea. *Journal of Marine Research*, *60*(4), 537–549. https://doi.org/10.1357/002224002762324202

24. Hirschi, J. J.-M., Frajka-Williams, E., Blaker, A. T., Sinha, B., Coward, A., Hyder, P., et al. (2019). Loop Current Variability as Trigger of Coherent Gulf Stream Transport Anomalies. *Journal of Physical Oceanography*, *49*(8), 2115–2132. https://doi.org/10.1175/JPO-D-18-0236.1

25. Hu, C, Montgomery, E., Schmitt, R., & Mullerkarger, F. (2004). The dispersal of the Amazon and Orinoco River water in the tropical Atlantic and Caribbean Sea: Observation from space and S-

311 PALACE floats. *Deep Sea Research Part II: Topical Studies in Oceanography*, *51*(10–11), 1151–
312 1171. https://doi.org/10.1016/S0967-0645(04)00105-5
313 26. Hu, Chuanmin, Nelson, J. R., Johns, E., Chen, Z., Weisberg, R. H., & Müller-Karger, F. E. (2005).
314 Mississippi River water in the Florida Straits and in the Gulf Stream off Georgia in summer 2004:
315 MISSISSIPPI WATER IN THE FLORIDA STRAITS. *Geophysical Research Letters*, *32*(14), n/a-n/a.
316 https://doi.org/10.1029/2005GL022942
317 27. Jouanno, J., Sheinbaum, J., Barnier, B., Molines, J.-M., Debreu, L., & Lemarié, F. (2008). The
318 mesoscale variability in the Caribbean Sea. Part I: Simulations and characteristics with an embedded
319 model. *Ocean Modelling*, *23*(3–4), 82–101. https://doi.org/10.1016/j.ocemod.2008.04.002
320 28. Killworth, P. D. (2004). Physical and biological mechanisms for planetary waves observed in satellite-
321 derived chlorophyll. *Journal of Geophysical Research*, *109*(C7), C07002.
322 https://doi.org/10.1029/2003JC001768
323 29. Liu, Y., Weisberg, R. H., Hu, C., & Zheng, L. (2011). Trajectory Forecast as a Rapid Response to the
324 Deepwater Horizon Oil Spill. In Y. Liu, A. MacFadyen, Z.-G. Ji, & R. H. Weisberg (Eds.),
325 *Geophysical Monograph Series* (Vol. 195, pp. 153–165). Washington, D. C.: American Geophysical
326 Union. https://doi.org/10.1029/2011GM001121
327 30. Liu, Y., Weisberg, R. H., Vignudelli, S., & Mitchum, G. T. (2016). Patterns of the loop current system
328 and regions of sea surface height variability in the eastern Gulf of Mexico revealed by the self-
329 organizing maps. *Journal of Geophysical Research: Oceans*, *121*(4), 2347–2366.
330 https://doi.org/10.1002/2015JC011493
331 31. Maritorena, S., d'Andon, O. H. F., Mangin, A., & Siegel, D. A. (2010). Merged satellite ocean color
332 data products using a bio-optical model: Characteristics, benefits and issues. *Remote Sensing of*
333 *Environment*, *114*(8), 1791–1804. https://doi.org/10.1016/j.rse.2010.04.002
334 32. Muller-Karger, F., McClain, C. & Richardson, P. The dispersal of the Amazon's
335 water. Nature 333, 56–59 (1988). https://doi.org/10.1038/333056a0

33. Murphy, S. J., Hurlburt, H. E., & O'Brien, J. J. (1999). The connectivity of eddy variability in the Caribbean Sea, the Gulf of Mexico, and the Atlantic Ocean. *Journal of Geophysical Research: Oceans*, *104*(C1), 1431–1453. https://doi.org/10.1029/1998JC900010

34. O'Brien, R. C., Cipollini, P., & Blundell, J. R. (2013). Manifestation of oceanic Rossby waves in long-term multiparametric satellite datasets. *Remote Sensing of Environment*, *129*, 111–121. https://doi.org/10.1016/j.rse.2012.10.024

35. Oey, Lie-Yauw. (2004). Vorticity flux through the Yucatan Channel and Loop Current variability in the Gulf of Mexico. *Journal of Geophysical Research*, *109*(C10), C10004. https://doi.org/10.1029/2004JC002400

36. Oey, L.-Y., Ezer, T., & Lee, H.-C. (2005). Loop Current, Rings and Related Circulation in the Gulf of Mexico: A Review of Numerical Models and Future Challenges. In Wilton Sturges & A. Lugo-Fernandez (Eds.), *Geophysical Monograph Series* (pp. 31–56). Washington, D. C.: American Geophysical Union. https://doi.org/10.1029/161GM04

37. Pujol, M.-I., Faugère, Y., Taburet, G., Dupuy, S., Pelloquin, C., Ablain, M., & Picot, N. (2016). DUACS DT2014: the new multi-mission altimeter data set reprocessed over 20years. *Ocean Science*, *12*(5), 1067–1090. https://doi.org/10.5194/os-12-1067-2016

38. Richardson, P. L. (2005). Caribbean Current and eddies as observed by surface drifters. *Deep Sea Research Part II: Topical Studies in Oceanography*, *52*(3–4), 429–463. https://doi.org/10.1016/j.dsr2.2004.11.001

39. Shay, L. K., & Jacob, S. D. (2006). Relationship between oceanic energy fluxes and surface winds during tropical cyclone passage. In W. Perrie (Ed.), *WIT Transactions on State of the Art in Science and Engineering* (1st ed., Vol. 1, pp. 115–142). WIT Press. https://doi.org/10.2495/978-1-85312-929-2/05

40. Sheng, Y. P., Zhang, Y., & Paramygin, V. A. (2010). Simulation of storm surge, wave, and coastal inundation in the Northeastern Gulf of Mexico region during Hurricane Ivan in 2004. *Ocean Modelling*, *35*(4), 314–331. https://doi.org/10.1016/j.ocemod.2010.09.004

41. Sturges, W. (2000). Frequency of Ring Separations from the Loop Current in the Gulf of Mexico: A Revised Estimate. *JOURNAL OF PHYSICAL OCEANOGRAPHY*, *30*, 6.

42. Weisberg, R. H., & Liu, Y. (2017). On the Loop Current Penetration into the Gulf of Mexico. *Journal of Geophysical Research: Oceans*, *122*(12), 9679–9694. https://doi.org/10.1002/2017JC013330

43. Weisberg, R.H., L. Zheng, and Y. Liu (2017). On the Movement of Deepwater Horizon Oil to Northern Gulf Beaches. *Ocean Modelling,* 111, 81-97. https://doi.org/10.1016/j.ocemod.2017.02.002

44. Weisberg, R. H., Zheng, L., Liu, Y., Murawski, S., Hu, C., & Paul, J. (2016). Did Deepwater Horizon hydrocarbons transit to the west Florida continental shelf? *Deep Sea Research Part II: Topical Studies in Oceanography*, *129*, 259–272. https://doi.org/10.1016/j.dsr2.2014.02.002

45. van Westen, R. M., Dijkstra, H. A., Klees, R., Riva, R. E. M., Slobbe, D. C., van der Boog, C. G., et al. (2018). Mechanisms of the 40-70 Day Variability in the Yucatan Channel Volume Transport. *Journal of Geophysical Research: Oceans*, *123*(2), 1286–1300. https://doi.org/10.1002/2017JC013580

46. Xu, F.-H., Chang, Y.-L., Oey, L.-Y., & Hamilton, P. (2013). Loop Current Growth and Eddy Shedding Using Models and Observations: Analyses of the July 2011 Eddy-Shedding Event*. *Journal of Physical Oceanography*, *43*(5), 1015–1027. https://doi.org/10.1175/JPO-D-12-0138.1

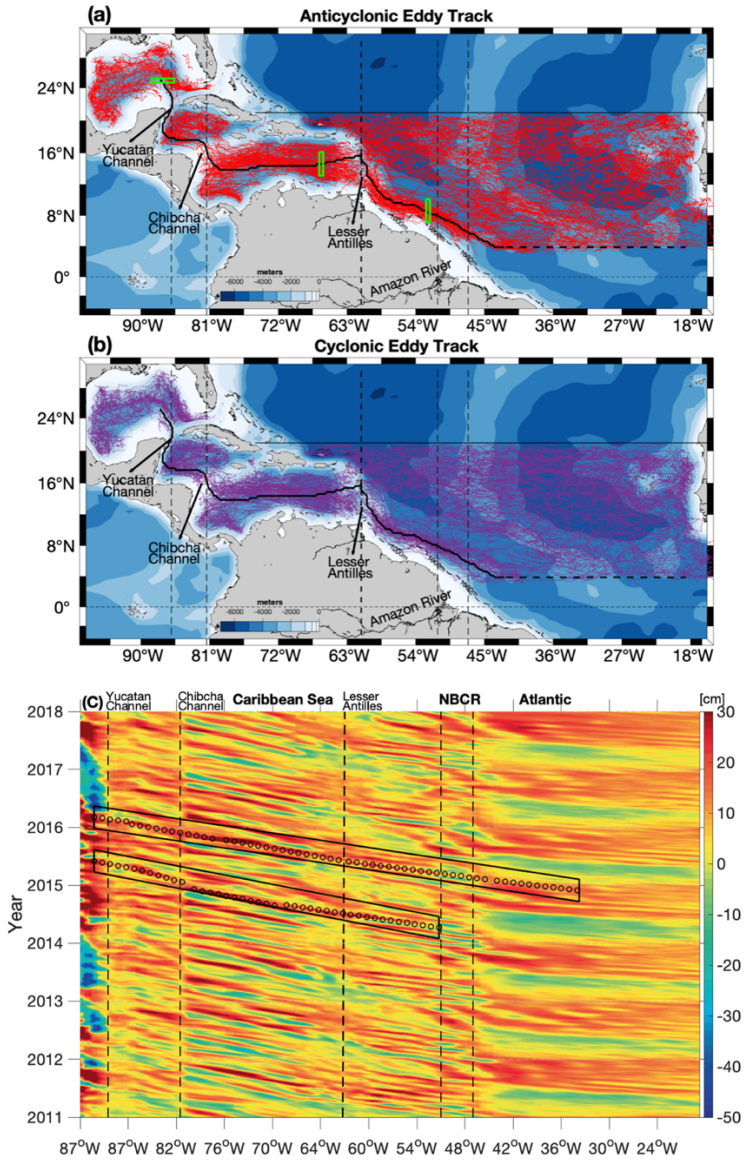

381

382 Fig. 1 Eddy tracks of (a) Anticyclonic eddies, (b) Cyclonic eddies in the study region. Only the
383 eddies last more than 60 days are shown. The black line stands for the mean eddy trajectory,
384 which is used to further examine the eddy propagation. The 1000m isobath is marked in the
385 North Brazil and the bathymetry is superimposed. (c) Time-longitude plot of SLA following the
386 mean eddy trajectory marked above from 2011 to 2018. The circle and the box from 2014 to
387 2016 mark the two eddy propagation cases. The dash lines mark the Lesser Antilles, Chibcha
388 Channel, Yucatan Channel and, NBC retroflection.

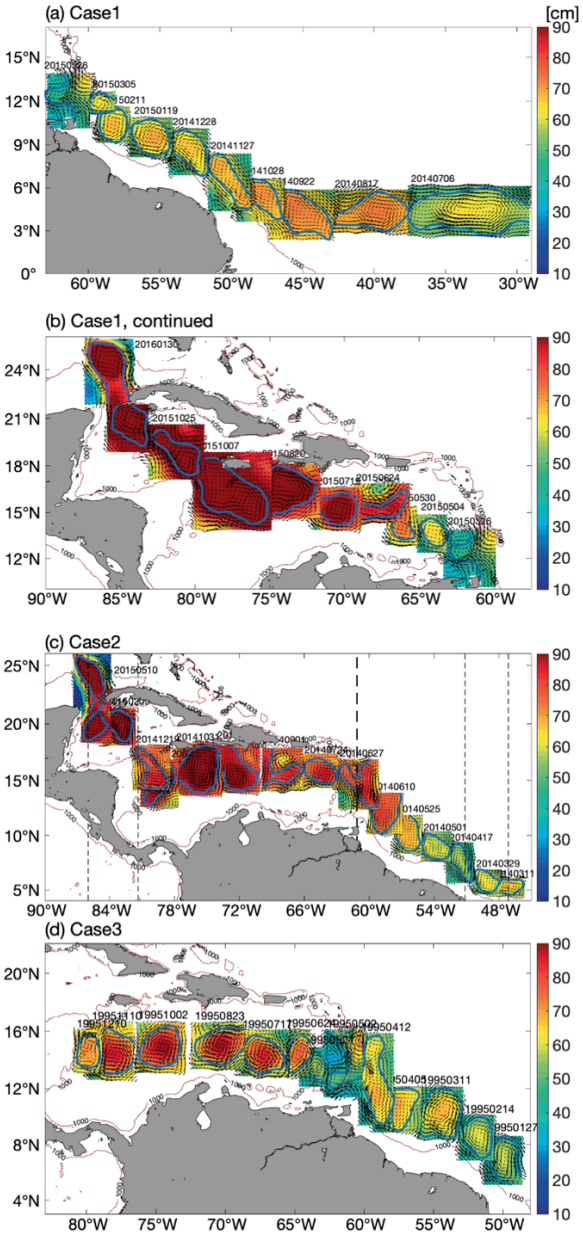

389

390 Fig. 2 Cases of long-distance propagation of individual eddy: (a-b) from July 2014 to January
391 2016, (c) from March 2014 to May 2015, and (d) from January 1995 to December 1995. The
392 dates are shown on the top of each snapshot. The absolute dynamic topography (ADT) is
393 superimposed by the geostrophic current and the outmost contour of ADT marks its boundary.
394 The 1000m isobath is marked.

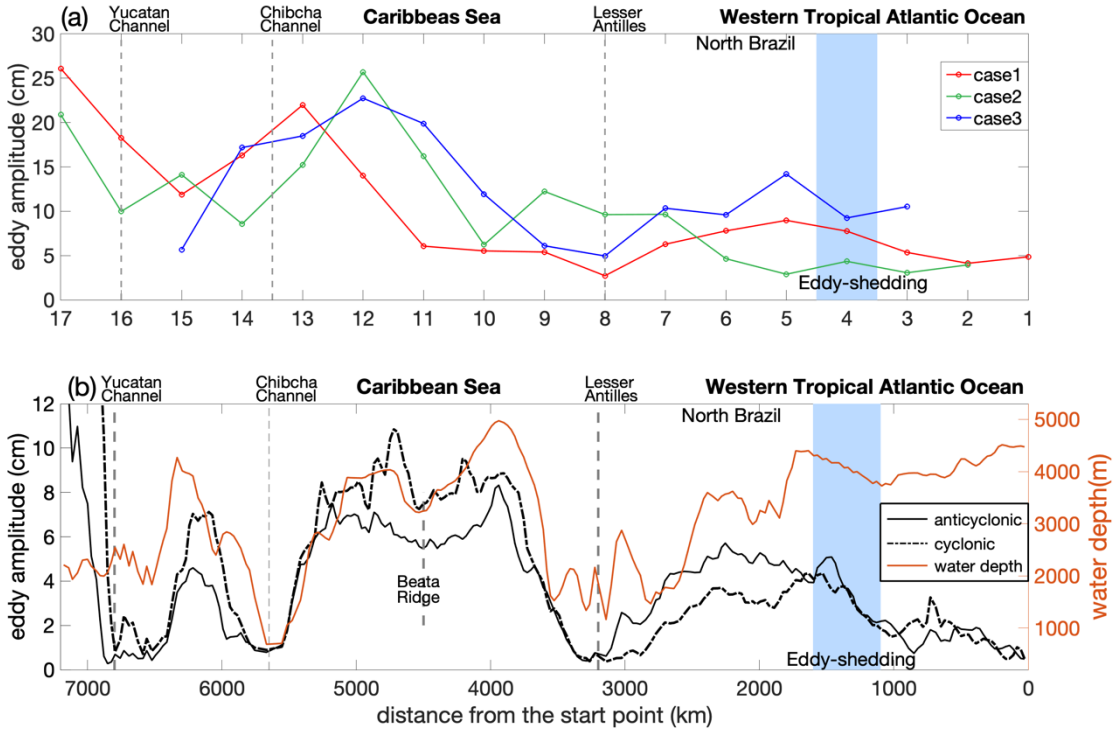

395

396 Fig. 3 (a) Eddy amplitude evolution (magnitude of the height difference between the extremum
397 of ADT within the eddy and the ADT around the contour shown in figure 2) for the three cases.
398 (b) Black solid line: eddy amplitude (magnitude of the height difference between the extremum
399 of SLA within the eddy and the SLA around the contour defining the eddy perimeter) evolution
400 for all the anticyclonic eddy cases following the line in Fig. 1a. Black dashed line: same as black
401 solid line, but for cyclonic eddies. The blue patch marks the eddy-shedding position. The
402 position of the Lesser Antilles, the Chibcha Channel, the Yucatan Channel and the Beata Ridge
403 is marked in dash lines. Orange line: the topography evolution following the line in Fig. 1a.

404

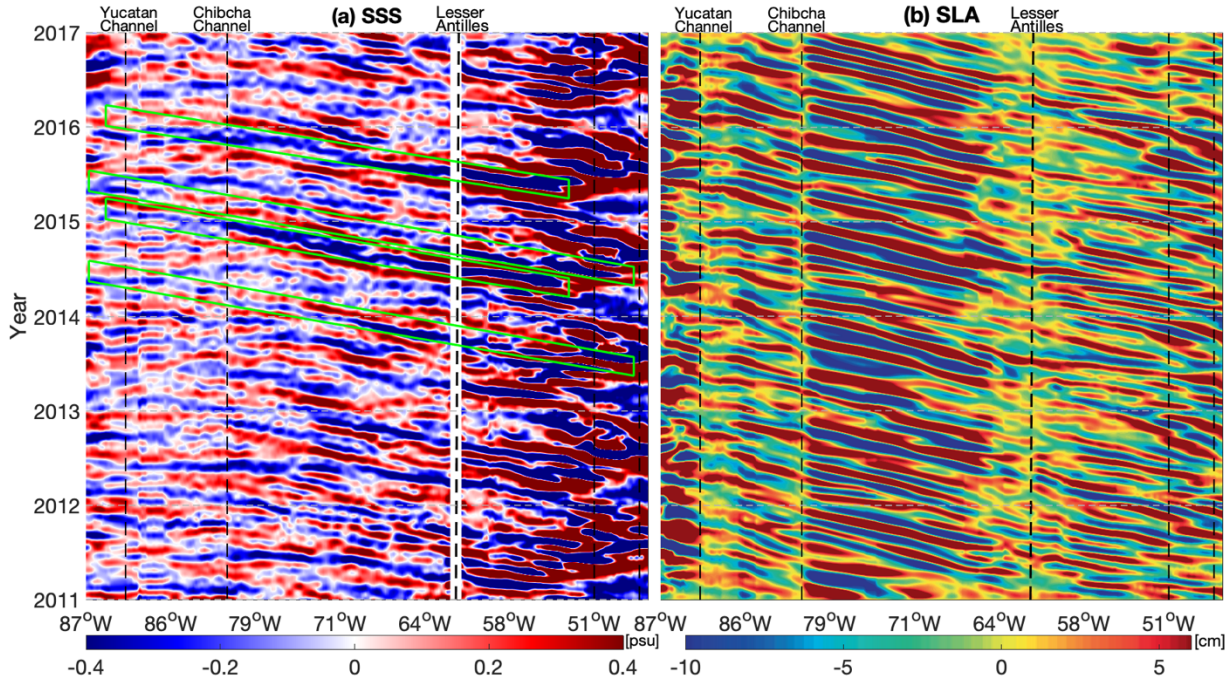

405

406 Fig. 4 Longitude-time plot of (a) sea surface salinity (SSS) anomalies and (b) sea level anomalies

407 (SLA) band-pass filtered between 40 and 200 days. The green boxes represent relatively

408 consistent signal propagate from NBC to GoM.

409

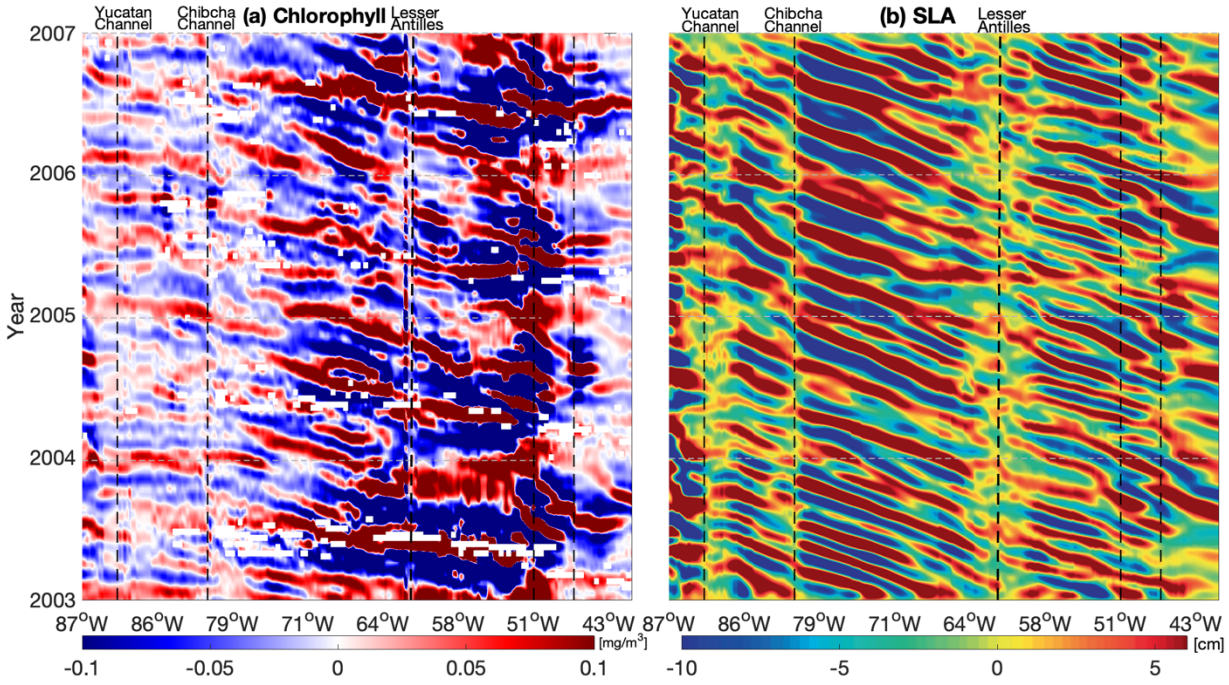

410

411 Fig. 5 Longitude-time plot of (a) chlorophyll anomalies and (b) sea level anomalies (SLA) band-

412 pass filtered between 40 and 200 days from 2003 to 2007. For clear, the chlorophyll data on the

413 left side of Lesser Antilles is doubled.